Area selection for diamonds using magnetotellurics: Examples from southern Africa

Alan G. Jones[1], Rob L. Evans[2], Mark R. Muller[1], Mark P. Hamilton[1,10,13], Marion P. Miensopust[1,14], Xavier Garcia[1,15], Patrick Cole[3], Tiyapo Ngwisanyi[4], David Hutchins[5], C.J. Stoffel Fourie[6], Heilke Jelsma[7], Theo Aravanis[8], Wayne Pettit[9], Sue Webb[10], Jan Wasborg[11], and The SAMTEX Team[12]

1: Dublin Institute for Advanced Studies, 5 Merrion Square, Dublin, Ireland;

2: Department of Geology and Geophysics, Woods Hole Oceanographic Institution, Clark South 172, 360 Woods Hole Road, Woods Hole, Massachusetts, 02543-1542, U.S.A.;

3: Council for Geoscience, 280 Pretoria Street, Silverton, Pretoria 0001, South Africa;

4: Geological Survey of Botswana, Private Bag 14, Lobatse, Botswana;

5: Geological Survey of Namibia, 1 Aviation Road, Windhoek, Namibia;

6: Council for Scientific and Industrial Research, Pretoria, South Africa;

7: De Beers Group Services, Private Bag X01, Southdale 2135, South Africa;

8: Rio Tinto Exploration,1 Research Avenue, Bundoora, 3081, Victoria, Australia;

9: BHP Billiton, Johannesburg, South Africa;

10: The University of the Witwatersrand, Jan Smuts Avenue, Johannesburg 2050, South Africa;

11: ABB AB, HVDC, Ludvika, SE-77180, Sweden;

12: Other members of the SAMTEX team include: Louise Collins, Colin Hogg, Clare Horan, Jessica Spratt, Gerry Wallace (DIAS), Alan D. Chave (WHOI), Janine Cole, Raimund Stettler (CGS), G. Tshoso (GSB), Andy Mountford, Ed Cunion (RTME), David Khoza (DIAS and BHP-B) and Pieter-Ewald Share (DIAS and CSIR);

13: Now at EMGS, Stiklestadveien 1, N-7041 Trondheim, Norway;

14: Registered at National University of Ireland, Galway;

15: Now at Institut de Ciències del Mar (CSIC), Barcelona, Spain

Corresponding author: Alan G. Jones. Email: alan@cp.dias.ie

Word Count: 6,742 Display Items: 9 colour figures

Abstract

Southern Africa, particularly the Kaapvaal Craton, is one of the world's best natural laboratories for studying the lithospheric mantle given the wealth of xenolith and seismic data that exist for it. The Southern African Magnetotelluric Experiment (SAMTEX) was launched to complement these databases and provide further constraints on physical parameters and conditions by obtaining information about electrical conductivity variations laterally and with depth. Initially it was planned to acquire magnetotelluric data on profiles spatially coincident with the Kaapvaal Seismic Experiment, however with the addition of seven more partners to the original four through the course of the experiment, SAMTEX was enlarged from two to four phases of acquisition, and extended to cover much of Botswana and Namibia. The complete SAMTEX dataset now comprises MT data from over 675 distinct locations in an area of over one million square kilometres, making SAMTEX the largest regional-scale MT experiment conducted to date.

Preliminary images of electrical resistivity and electrical resistivity anisotropy at 100 km and 200 km, constructed through approximate one-dimensional methods, map resistive regions spatially correlated with the Kaapvaal, Zimbabwe and Angola Cratons, and more conductive regions spatially associated with the neighbouring mobile belts and the Rehoboth Terrain. Known diamondiferous kimberlites occur primarily on the boundaries between the resistive or isotropic regions and conductive or anisotropic regions.

Comparisons between the resistivity image maps and seismic velocities from models constructed through surface wave and body wave tomography show spatial correlations between high velocity regions that are resistive, and low velocity regions that are conductive. In particular, the electrical resistivity of the sub-continental lithospheric mantle of the Kaapvaal Craton is determined by its bulk parameters, so is controlled by a bulk matrix property, namely temperature, and to a lesser degree by iron content and composition, and is not controlled by contributions from interconnected conducting minor phases, such as graphite, sulphides, iron oxides, hydrous minerals, etc. This makes quantitative correlations between velocity and resistivity valid, and a robust regression between the two gives an approximate relationship of Vs [m/s] = 0.045*log(resistivity [ohm.m]).

Key Words

Sub-continental lithospheric mantle, cratonic lithosphere, electrical conductivity, Kaapvaal Craton, Zimbabwe Craton, diamond exploration

1. Introduction

Only through high-resolution geophysical mapping of the sub-continental lithospheric mantle (SCLM) coupled with petrological and geochemical information from mantle xenoliths will we be able to understand its formation, deformation and destruction processes. The structure, geometry and observable in-situ physical parameters (seismic velocities and electrical conductivity) of the SCLM are reasonably well-known in some places, but incompletely known to unknown in many others. This disparity in knowledge is particularly acute for Southern Africa, where the seismic properties of the lithosphere beneath South Africa are well-known, but its electrical properties were not, and in sharp contrast the physical properties of the lithosphere beneath Botswana and Namibia were completely *Terra Incognita* prior to our work. In parallel to this academic quest, the diamond exploration community was interested in assessing the role that deep-probing electromagnetic surveying, using the magnetotelluric technique (MT), can play in area selection for diamond exploration activities, particularly when combined and contrasted with results from teleseismic experiments.

The electrical conductivity of the continental upper mantle is highly sensitive to ambient temperature (e.g., Jones, 1999a; Ledo and Jones, 2005; Jones et al., 2009), to iron content (given by magnesium number, Mg#) (Jones et al., 2009), to the presence of an interconnected conducting phase, such as a solid phase like graphite or sulphides (e.g., Duba and Shankland, 1982; Ducea and Park, 2000; Jones et al., 2003) or a fluid phase like partial melt (e.g., Park and Ducea, 2003), or to bound water through hydrogen diffusion (e.g., Karato, 1990, 2006; Hirth et al., 2000). Given these sensitivities, deep-probing magnetotellurics (MT) can aid in area selection for potential diamondiferous prospective regions by mapping regions with deep lithospheric roots and by mapping mantle regions above the graphite-diamond stability field that possibly contain high quantities of carbon (Jones and Craven, 2004).

The magnetotelluric technique is a natural-source electromagnetic method that was proposed theoretically in the early 1950s and has developed over half a century to become a sophisticated lithospheric geological mapping tool. Magnetotellurics involves recording simultaneously on the surface of the Earth the time-varying horizontal orthogonal components of the electric and magnetic fields, and deriving an Earth response function that contains information about the vertical and lateral variations in electrical resistivity. The interested reader is referred to a number of standard texts on the subject, including Jones (1999a), Simpson and Bahr (2005), and Vozoff’s (1986) compilation of older publications.

The MT results from the Archean Slave craton in NW Canada, with the identification of an upper mantle conductor – the Central Slave Mantle Conductor (Jones et al., 2001, 2003) – lying directly beneath the Eocene kimberlite field (Fipke’s so-called Corridor of Hope, Krajick, 2001) and also spatially and in depth collocated with an ultra-depleted high Mg# upper lithospheric harzburgitic region (Griffin et al., 1999), were exciting, interesting and intriguing, not only in terms of geometric controls that could be used in hypothesizing tectonic scenarios for the development of the sub-cratonic lithospheric mantle of the Slave craton (Davis et al., 2003) but also in terms of diamond exploration potential using MT. Through other deep-probing MT studies in Canada, the Slave’s CSMC was shown not to be as unique as first thought as similar conductors have also been found in the lithosphere of the Sask craton (Jones et al., 2005a), directly beneath one of the largest known kimberlite clusters in the world, the Fort-à-la-Corne kimberlite (Jones et al., 2005a), and beneath the western part of the Superior craton (Craven et al., 2001), where kimberlites have yet to be found.

These results begged for an MT study of the Kaapvaal Craton, the best-known geochemically in the world and also the best known seismically as a consequence of the Kaapvaal Craton Project. For the last 5 years, the Southern African Magnetotelluric Experiment (SAMTEX) project has been imaging the three-dimensional regional lithospheric-scale geometry of the electrical conductivity of the continental lithosphere below southern Africa. Herein we present the first regional images of electrical resistivity (inverse of conductivity) at lithospheric depths, and compare the inferred resistivities with kimberlite information and with seismic parameters at the same depths obtained from body wave and surface wave data from the Kaapvaal Seismic Experiment. From these images we draw inferences about diamond prospectivity in Southern Africa, and demonstrate the utility of magnetotellurics for efficient and effective area selection.

2. The SAMTEX project

During the mid-1990s and later there was interest expressed by some diamond exploration companies in the capabilities of deep-probing magnetotellurics as an effective area selection tool for diamondiferous regions, particularly for imaging the base of the lithosphere – the lithosphere-asthenosphere boundary (LAB). This interest grew as the diamond exploration community became more aware of the potential of the MT method through presentations (Jones, 1997; Jones, 2000; Jones and Craven, 2001) and short courses (Jones, 1999a; Jones, 2001), and as the results from the MT studies on the Slave craton came out (Jones, 1999b; Jones and Ferguson, 1998; Jones et al., 2001, 2003), particularly with the serendipitous mapping of the Central Slave Mantle Conductor (CSMC) – see Introduction.

In November, 2002 a proposal was submitted to the Continental Dynamics programme of the National Science Foundation (NSF) led by Rob Evans (WHOI) with four SAMTEX partners from academia, government and industry (see Acknowledgements). The proposal was for a relatively simple experiment to acquire data along two orthogonal profiles in predominantly South Africa during two phases of acquisition (black profiles in Fig. 1). The project was intended to cover the same area as the Southern African Seismic Experiment (SASE) array (black dots in Fig. 1) of the Kaapvaal Craton Project, with overarching aims of determining the resistivity structure of the Kaapvaal craton and comparing and contrasting it to the seismic models of the craton and also with the resistivity structure of other cratons. The proposal was funded in Spring, 2003 with the first phase of fieldwork taking place in Autumn, 2003. Besides NSF, other funding came from DeBeers and from a South African Department of Science and Technology grant to the Council for Geoscience. As the SAMTEX project progressed, more partners joined the consortium, which now comprises a total of eleven members (see Acknowledgements). We have now completed four far larger phases of acquisition, rather than the two originally planned (compare black profiles to actual station locations in Fig. 1), and in addition, DeBeers donated proprietary MT data to the SAMTEX project (yellow sites in Fig. 1). In total, the SAMTEX dataset now comprises data from a total of more than 730 sites along ~14,000 line kilometres over an area in excess of a million square kilometres. As such, this is by far the largest regional-scale MT project ever undertaken.

The electric and magnetic time series recorded at each location were processed into MT responses using robust methods, namely improved versions of methods 6, 7 and 8 in Jones et al. (1989). Data quality was generally very high, especially in Namibia and Botswana, but was poor at some locations in South Africa, particularly close to the town of Kimberley and in the Witwatersrand Basin, due to the high amplitude electrical-noise generated by the DC power-supply to both the mines and railway lines.

3. Map construction

Preliminary qualitative information on regional-scale resistivity variations can be obtained rapidly from the magnetotelluric impedance tensors at each station through constructing maps of various parameters. Conventionally, these maps are created at specific periods thought to be penetrating to crustal or mantle depths. However such fixed-period maps can be highly misleading if crustal conductivity varies significantly across the region, a problem that is extreme for southern Africa (Hamilton et al., 2006; Jones, 2006). For example, along the 2003 main NE-SW Kaapvaal craton profile (red circles in Fig. 1) electromagnetic (EM) waves at periods of around 1 second penetrate to the base of the crust at stations in the centre of the craton but for the same penetration depth periods of 1,000 seconds or greater are needed at the SW end on the Namaqua-Natal mobile belt due to the presence of highly conducting layers in the crust, including the Whitehill Formation (Branch et al., 2007). Thus, it is necessary to perform an approximate depth conversion prior to constructing the maps, which is done here using the Niblett-Bostick (NB) transform from apparent resistivity and phase against period to layer resistivity against depth (Niblett and Sayn Wittgenstein, 1960; Bostick, 1977; Jones, 1983; Vozoff, 1986); more explanation can be found in Jones et al. (2005a, 2005b).

It must be appreciated that these maps are images of the actual resistivity distribution; they are not models constructed through either a forward data-fitting exercise or application of a formal inversion of the data for the resistivity model. It must also be appreciated that these images are formed from a 1-D approximation applied to a 2-D or 3-D world, and the results are to be taken in a qualitative manner, rather than a quantitative one. Finally, static shifts (Jones, 1988) of the magnetotelluric magnitudes are treated through spatial averaging with outlier rejection. Notwithstanding these caveats, dominant robust features in the images have been verified through more formal multi-dimensional modelling of some of the profiles (see, e.g., Muller et al., 2009).

We show image maps of estimated bulk resistivity and a measure of anisotropy for certain depths, and a map of the integrated conductivity between two depth ranges. The depths we have chosen for bulk resistivity and anisotropy are 100 km and 200 km. The first approximates the middle of the lithosphere and the second approximates the base of the lithosphere. For integrated conductivity we show the depth range of 40-200 km, i.e., the mantle lithosphere.

For bulk resistivity the parameter we choose to present is the maximum resistivity for each site at the given depth. This is obtained by rotating the apparent resistivity and phase data through 180°, deriving the NB transformed resistivity-depth data, and determining the largest value of resistivity at the particular depth of interest. This maximum resistivity is robust in that it is only affected by significant conductivity bodies and is less affected by distortion effects, and it will lead to conservative maps. Note that the maximum resistivity is not solely one of the two-dimensional modes of induction in MT, namely the transverse electric (TE) or transverse magnetic (TM) mode. On the conductive side of a contact between two media of different resistivity, the maximum resistivity is the TE mode, whereas on the resistive side of a contact, it is the TM mode.

An estimate of the sensitivity of the maximum resistivity to strike direction is obtained from mapping electrical anisotropy. Electrical anisotropy can be interpreted in terms of either macro, i.e., structural (two- or three-dimensionality), or micro, i.e., grain boundary, anisotropy; other information must be used to distinguish between these two. Formally this is done through consideration of the rotation properties of the MT impedance tensor and using a tensor decomposition approach (e.g., McNeice and Jones, 2001; Hamilton et al., 2006; Hamilton, 2008), but here we use an approximate method. The anisotropy at a given depth we derive from determining the maximum NB resistivity at that depth, and determining the NB resistivity in the direction 90° from it, and computing the anisotropy as:

$$\text{anisotropy} = \log(\rho_{NB}(h,\Theta_{\max})) - \log(\rho_{NB}(h,\Theta_{\max}+90)) \quad .$$

Note that this value is derived from NB resistivities at different periods, following the concerns expressed by Jones (2006) in situations where penetration by EM fields is different in orthogonal directions. Thus it does offer some advantages over the more formal methods that can suffer from problems discussed by Jones (2006). For this value to be computed there has to be penetration to the required depth in both the *RhoMAX* direction (Θ_{max}) and also the direction perpendicular to it (which may or may not be the *RhoMIN* direction). An anisotropy value of 1 means that $log_{10}(RhoMAX)$ is one decade larger than $log_{10}(RhoMIN)$, so a factor of 10 larger.

Finally, the depth-integrated conductivity, or conductance (S) in Siemens (S), value for each site and the mantle lithospheric depth range is derived by converting the NB resistivity-depth profile into a layered Earth profile and then summing the conductances of each layer between the depths of interest.

The maps of Southern Africa displaying electrical parameters were generated from the SAMTEX database using the GMT, Generic Mapping Tools (Wessel and Smith, 1991; 1998). Maps of the same or similar responses for specific regions have been presented in the past for southern British Columbia, Canada (Jones and Gough, 1995), the Trans-Hudson Orogen (Jones et al., 2005a), and the SNORCLE transect region in northwestern Canada (Jones et al., 2005b), and the same procedures are followed here. The parameters are $\log_{10}$(NB resistivity), anisotropy, and conductance. The steps involved in making the maps are:

1. Spatial smoothing using median filter routine *blockmedian* with an increment of 30 minutes.
2. Creating an interpolated grid from the median smoothed data using a continuous curvature gridding algorithm *surface* with a 10 minute grid spacing and a tension of 0.5.
3. Plotting using *grdimage*.

The data used for the maps do not include the sites from the Southern Cross (blue Phase II sites in the SE part of the Kaapvaal Craton in Fig. 1), due to noise issues related to DC trains and major pipelines that have yet to be overcome, nor from the Phase IV sites in South Africa (purple RSA sites in Fig. 1) due to confidentiality restrictions.

4. Electrical maps

4.1 100 km and 200 km depth resistivity maps

The maps of the maximum (NB) resistivity at (NB) depths of 100 km and 200 km are shown in Figs. 2 and 3 respectively. Mantle lithospheric rocks comprising olivine, pyroxenes and garnet at lithospheric mantle P-T conditions appropriate for the Kaapvaal Craton should have resistivities of the order of 30,000 Ω.m or greater at 100 km (P-T conditions of 3.0 GPa and 740 °C) and of the order of 1,000 Ω.m at 200 km (P-T conditions of 6.3 GPa and 1250 °C) (Ledo and Jones, 2005; Jones et al., 2009). The hotter colours, yellows to reds, are indicative of either hotter conditions and/or the presence of conducting components.

The maps show a very resistive core region of significant spatial extent that is spatially associated with the Kaapvaal Craton. In particular there is strong correlation between the northwestern boundary of the Kaapvaal Craton, as mapped on the surface, and the edge of the high resistivity body. The northeastern part of the Kaapvaal Craton shows lower resistivity, and the more conductive regions spatially coincide with the mapped boundaries of the surface exposures of the Bushveld Complex (Fig. 1). The Bushveld

Complex is thought to have affected the seismic structure of the craton, with lower velocities in the mantle (James et al., 2001), and in our data there is evidence of an effect on electrical conductivity. Resistive deep lithosphere is spatially associated with the Angola Craton (Fig. 3) and with parts of the Zimbabwe Craton, especially its westward tongue on which the Orapa kimberlite field lies (Fig. 3).

Our data shown here, and the formal inversion models shown in Muller et al. (2009), give evidence for low resistivity for the Rehoboth Terrain, thought by some to be an Archean craton. The Rehoboth Terrain does not exhibit the very high resistivity associated with Archean cratons and we conclude that the lithosphere-asthenosphere boundary is shallow – with a maximum value of the order of 180 km at most (Muller et al., 2009), which is close to the graphite-diamond phase transition.

On the 200 km depth map (Fig. 3) are also plotted the known kimberlite localities, and they are colour-coded according to whether the kimberlite is known to be diamondiferous (red), known to be non-diamondiferous (green) or either unknown (to us!) or undefined (white). There is an obvious spatial correlation between the edges of resistive regions and diamondiferous kimberlites. One strikingly anomalous occurrence is the purported diamondiferous kimberlite in the Rietfontein cluster on the Namibian/South African border, but this is now known to be a *bicycle diamond*, i.e., the diamonds did not originate from that kimberlite pipe but were brought in from elsewhere.

4.2 100 km and 200 km depth anisotropy maps

Figures 4 and 5 show the electrical anisotropy at depths of 100 km and 200 km respectively. Regions that are cold coloured (purple to blue) show little electrical anisotropy (less than an order of magnitude) whereas hotter coloured regions (yellow to pink to white) are evidence of high electrical anisotropy (one and a half orders of magnitude or more). At

100 km the region outlined as the Rehoboth Terrain is remarkably isotropic, and this isotropy persists to 200 km, although it diminishes in spatial extent. The isotropic region extends eastwards to the eastern half of the Okwa Terrane and along the Magondi Mobile Belt. In contrast, the cratonic regions are highly anisotropic – evidence of strong lateral heterogeneity. Interestingly, in Botswana the diamondiferous kimberlites lie on the edges of the isotropic region (Fig. 5), but this relationship is not upheld in South Africa.

4.3 Lithospheric conductance

The map of lithospheric conductance is shown in Fig. 6. For cratonic conditions, olivine-pyroxene-garnet compositions will result in a conductance of the order of 10 Siemens (Ledo and Jones, 2005; Jones et al., 2009), denoted by purple in the figure (note that the colour scale is logarithmic). The central core of the Kaapvaal Craton is generally as resistive as expected for dry cratonic conditions (Jones et al., 2009) through much of its depth extent. This is in sharp contrast to the Slave Craton (Jones et al., 2003), the Sask Craton (Jones et al., 2005a), and the western part of the Superior Craton (Craven et al., 2001), all of which exhibit conductivity anomalies in the upper lithospheric mantle, and in the case of the Slave and Sask Cratons these anomalies are spatially coincident with major diamondiferous kimberlite fields – the Eocene-aged kimberlites in the Central Slave and the Fort-à-la-Corne kimberlites in Saskatchewan. These anomalously conductive regions in other cratonic regions show that mapping using electrical conductivity does require care as there is no single universal response.

For Southern Africa there is an obvious spatial relationship between diamondiferous kimberlites and the edge of resistive lithosphere for the Kaapvaal Craton. This relationship does not hold for the diamondiferous kimberlite fields discussed above as there is conducting material in the lithospheric columns.

5. Comparison with Kaapvaal Seismic Experiment results

Various groups have analysed the data from the Kaapvaal Seismic Experiment, and both body wave and surface wave models have been generated. Body wave models, for both compressional (P) and shear (S) wave arrivals, were derived by Matt Fouch (Fouch et al., 2004; James et al., 2001), and a surface wave model, using the fundamental mode only of Rayleigh waves, was derived by Aibing Li (Li and Burke, 2006).

5.1 Comparison with Surface Wave model at 100 km

As shown by Li and Burke (2006), the sensitivity kernels for surface wave methods are such that the deeper in the Earth one investigates, the more smearing occurs due to the broadening of the kernels. Figure 5 of Li and Burke (2006) shows that the resolution kernel for 50 s periodicity is centred on 80 km, and averages information from approximately the base of the crust (40 km) to approximately the graphite-diamond phase transition (140 km), thus this depth gives a weighted average of the 1-D vertical seismic velocity in the upper lithospheric mantle.

Figure 7 shows the velocities in the 80-100 km depth slice of the Li and Burke SW model, and can be directly compared qualitatively with the corresponding resistivity map at 100 km (Fig. 2). Also plotted on the figure are the kimberlite localities. As with electrical resistivity, there is a positive correlation of diamondiferous kimberlites with the edge of the high velocity body associated with the Kaapvaal Craton and also with the edge of the high velocity body associated with the Zimbabwe Craton. Formal correlation of these two maps, using linear regression with robust outlier rejection (Huber, 1981) and assuming that both data are in error (York, 1966, 1969; Fasano and Vio, 1988), yields the result that velocity and logarithm(resistivity) are related by approximately:

$$Vs = 0.045 * \log10(\rho) + 4.50 \quad m/s.$$

However, further work has to be undertaken to improve both the seismic images and the electrical ones in order to verify this relationship.

5.2 Comparison with Body Wave models at 200 km

The Vp and Vs perturbation anomaly maps at 200 km from the Fouch et al. (2004) models are shown in Figs 8 and 9 respectively, together with the resistivity map at that same depth (Fig. 3) and the kimberlite information. Velocity anomalies in the range ±0.25% are set to transparent, and positive velocity anomalies grade through blue to black (1.25%) and negative ones grade through red to black (-1.25%).

As with the Li and Burke map (Fig. 7), there is an obvious correlation of the boundaries of the high velocity anomaly associated with the Kaapvaal Craton. The fast velocity anomalies in both Vp and Vs spatially correlate well with high resistivity anomalies, and vice-versa. The one region that appears to contradict this central Botswana, which displays a low resistivity region (Fig. 3), no Vp anomaly (Fig. 8), but a relatively strong (0.5%) fast Vs anomaly (Fig. 9).

6. Conclusions

Maps of electrical resistivity and resistivity anisotropy derived from approximate methods give robust information about large-scale regional structures. These maps can be derived for various depths and compared with other information about the continental lithosphere, such as seismic velocities and information from kimberlites. In the case of southern Africa, the maps show evidence of obvious spatial correlations between diamondiferous kimberlite fields and lateral changes in either resistivity or resistivity anisotropy. These spatial correlations of gradients in physical parameters at the edges of cratons being the most prospective diamondiferous regions appear also to hold in seismic parameters.

Based on these results, we conclude that on a statistical basis area selection for diamond exploration activities should focus on the edges of cratons where there are gradients in velocity and electrical conductivity, rather than the centres of cratons. These gradients are indicative of rapid shallowing of the deep lithospheric roots, and suggest that either the kimberlite magmas are generally unable to penetrate through thick roots, or that the processes of initiation of kimberlitic eruptive magmas are preferentially at depths shallower than the thickest roots. This is a revision of Clifford´s Rule (Clifford, 1966) that implies that the thinner edges of cratons are more prospective than the thicker centres, a suggestion made previously by Griffin et al. (2004) based on the kimberlite distribution on the North American Plate. However, there are notable exceptions to this; for example the Victor kimberlite field in Atiwapiskat, central Superior Province of Canada in the Hudson's Bay lowlands, for which it has been proposed that the lithosphere was thermally weakened by the passage of the Monteregian hotspot (Eaton and Frederiksen, 2007).

For the Kaapvaal Craton there is the suggestion of a linear correlation between the logarithm of electrical resistivity and Vs seismic velocity, implying that electrical resistivity is controlled not by minor constituents, as is often the case, but by the primary rock matrix. As shown by Jones et al. (2009), for cratonic lithosphere comprising olivine, pyroxenes and garnet, temperature variation dominates the variation in resistivity, with a minor effect due to magnesium number and almost no sensitivity to other compositional parameters. Seismic velocities have about a 70% dependence on temperature, and the rest is due to Mg# and composition, so using seismic and electrical information taken together it may be possible to derive the composition, temperature and depletion of the mantle lithosphere.

7. Acknowledgments

The SAMTEX project was initially conceived in Summer, 1996 in telephone discussions between Alan Jones (then at the Geological Survey of Canada), Leo Fox (Phoenix Geophysics, Canada) and Eddie Kostlin (then with Anglo American). Also pertinent to SAMTEX being eventually launched was a 1998 meeting between Jones and Edgar Stettler (then Head of Geophysics at the South African Council for Geoscience) that led to what has proven to be an absolutely invaluable contribution from CGS through all four phases of SAMTEX. Three institutions and one company came together to initiate SAMTEX in 2002 and were the Dublin Institute for Advanced Studies (academia), Woods Hole Oceanographic Institution (academia), The Council for Geoscience (government), and De Beers Group Services (industry). Seven others joined SAMTEX during the four phases of acquisition, in chronological order; The University of the Witwatersrand (academia), Geological Survey of Namibia (government), Geological Survey of Botswana (government), Rio Tinto Mining and Exploration (industry), BHP Billiton (industry), Council for Scientific and Industrial Research of South Africa (government), and ABB Sweden (industry) for the Namibian Power Corporation (government).

Many, many, many people on three continents contributed to the huge achievement in data acquisition of the SAMTEX project. Besides the consortium members and their staffs, we wish to acknowledge Phoenix Geophysics's many timely contributions of equipment and spares, and the Geological Survey of Canada and the U.S. Electromagnetic Studies of Continents consortium (EMSOC) for access to instrumentation. We especially thank our academic funding sponsors; the Continental Dynamics programme of the U.S. National Science Foundation, the South African Department of Science and Technology, and Science Foundation Ireland.

We thank Matt Fouch and Aibing Li for making their models available to us.

Finally, we thank the people of Southern Africa for their generous warm spirit allowing weird scientists on their land.

References

Bostick, F.X., 1977. A simple almost exact method of MT analysis, Workshop on Electrical Methods in Geothermal Exploration. U.S.G.S., Contract No. 14080001 8 359, Reprinted in Vozoff (1986).

Branch, T., Ritter, O., Weckmann, U., Sachsenhofer, R.F., Schilling, F., 2007. The Whitehill Formation - a high conductivity marker horizon in the Karoo Basin. South African Journal of Geology 110 (2-3), 465-476.

Clifford, T.N., 1966. Tectono-metallogenic units and metallogenic provinces of Africa. Earth and Planetary Science Letters 1 (6), 421-434.

Craven, J.A., 2001. Towards a 3-D image of electrical lithosphere beneath the Western Superior Transect. Western Superior Transect Sixth Annual Workshop, Ottawa.

Davis, W.J., Jones, A.G., Bleeker, W., Grutter, H., 2003. Lithosphere development in the Slave craton: a linked crustal and mantle perspective. Lithos 71 (2-4), 575-589.

Duba, A.G., Shankland, T.J., 1982. Free carbon and electrical conductivity in the Earth's mantle. Geophysical Research Letters 9 (11), 1271-1274.

Ducea, M.N., Park, S.K., 2000. Enhanced mantle conductivity from sulfide minerals, southern Sierra Nevada, California. Geophysical Research Letters 27 (16), 2405-2408.

Eaton, D.W., Frederiksen, A., 2007. Seismic evidence for convection-driven motion of the North American plate. Nature 446 (7134), 428-431.

Fasano, G., Vio, R., 1988. Fitting a straight line with errors on both coordinates. Newsletter of Working Group for Modern Astronomical Methodology 7, 2-7.

Fouch, M.J., James, D.E., VanDecar, J.C., van der Lee, S., Kaapvaal Seismic Group, 2004. Mantle seismic structure beneath the Kaapvaal and Zimbabwe Cratons. South African Journal of Geology 107 (1-2), 33-44.

Griffin, W.L., Doyle, B.J. , Ryan, C.G., Pearson, N.J. , O'Reilly, S.Y., Davies, R., Kivi, K., Van Achterbergh, E., Natapov L.M., 1999. Layered mantle lithosphere in the Lac de Gras area, Slave Craton: Composition, structure and origin. Journal of Petrology 40 (5), 705-727.

Griffin, W.L., O'Reilly, S.Y., Doyle, B.J., Pearson, N.J., Coopersmith, H., Kivi, K., Malkovets, V., Pokhilenko, N., 2004. Lithosphere mapping beneath the north American plate. Lithos 77 (1-4), 873-922.

Hamilton, M.P., 2008. Electrical and seismic anisotropy of the lithosphere with the focus on central southern Africa. Ph.D. thesis, The University of the Witwatersrand, Johannesburg.

Hamilton, M.P., Jones, A.G., Evans, R.L., Evans, S., Fourie, C.J.S., Garcia, X., Mountford, A., Spratt, J.E., SAMTEX Team, 2006. Electrical anisotropy of South African lithosphere compared with seismic anisotropy from shear-wave splitting analyses. Physics of the Earth and Planetary Interiors, 158 (2-4), 226-239.

Hirth, G., Evans, R.L., Chave, A.D., 2000. Comparison of continental and oceanic mantle electrical conductivity: Is the Archean lithosphere dry? Geochemistry Geophysics Geosystems 1, doi: 2000GC000048.

Huber, P.J., 1981. Robust Statistics. John Wiley, New York, 308 pp.

James, D.E., Fouch, M.J., VanDecar, J.C., van der Lee, S., Kaapvaal Seismic Group, 2001. Tectospheric structure beneath southern Africa. Geophysical Research Letters 28 (13), 2485-2488.

Jones, A.G., 1983. On the equivalence of the Niblett and Bostick transformations in the magnetotelluric method. Journal of Geophysics-Zeitschrift Fur Geophysik 53 (1), 72-73.

Jones, A.G., 1988. Static shift of magnetotelluric data and its removal in a sedimentary basin environment. Geophysics 53 (7), 967-978.

Jones, A.G., 1997. Imaging the continental upper mantle using electromagnetic methods, Workshop on Continental Roots, Harvard, Cambridge, Mass., U.S.A.

Jones, A.G., 1999a. Imaging the continental upper mantle using electromagnetic methods. Lithos 48 (1-4), 57-80.

Jones, A.G., 1999b. Information about the continental mantle from deep electromagnetic studies, Short Course on Geophysical and Geochemical Imaging of Canada's Upper Mantle, Yellowknife, NWT, Canada.

Jones, A.G., 1999c. Slave EM, Yellowknife Geoscience Forum, Yellowknife, NWT, Canada.

Jones, A.G., 2000. Lighting up the mantle: Information from electromagnetic waves about the continental mantle lithosphere and asthenosphere (Invited), Cordilleran Roundup, Vancouver, B.C., Canada.

Jones, A.G., 2001. Information about the continental mantle from deep electromagnetic studies. In: A.G. Jones (Editor), One-day Short Course on Geophysical and Geochemical Imaging of Canada's Upper Mantle, Toronto, Ont., Canada.

Jones, A.G., 2006. Electromagnetic interrogation of the anisotropic Earth: Looking into the Earth with polarized spectacles. Physics of the Earth and Planetary Interiors 158 (2-4), 281-291.

Jones, A.G., Chave, A.D., Auld, D., Bahr, K., Egbert, G., 1989. A comparison of techniques for magnetotelluric response function estimation. Journal of Geophysical Research 94 (B10), 14,201-14,213.

Jones, A.G., Craven, J.A., 2001. Carbon in the mantle? The electromagnetic responses of the Slave and Superior cratons compared and contrasted, Yellowknife Geoscience Forum, Yellowknife, NWT, Canada.

Jones, A.G.. Craven, J.A., 2004. Area selection for diamond exploration using deep-probing electromagnetic surveying. Lithos 77 (1-4), 765-782.

Jones, A.G., Evans, R.L., Eaton, D.W., 2009. Velocity-conductivity relationships for mantle mineral assemblages in Archean cratonic lithosphere based on a review of laboratory data and application of extremal bound theory. Lithos 109 (1-2), 131-143.

Jones, A.G., Ferguson, I.J., 1998. Northern lights and diamonds: Imaging the Slave cratonic lithosphere using very long period electromagnetic experiments, Yellowknife Geoscience Forum, Yellowknife, NWT, Canada.

Jones, A.G., Ferguson, I.J., Chave, A.D., Evans, R.L., McNeice, G.W., 2001. The electric lithosphere of the Slave craton. Geology 29 (5), 423-426.

Jones, A.G., Gough, D.I., 1995. Electromagnetic images of crustal structures in southern and central Canadian Cordillera. Canadian Journal of Earth Sciences 32 (10), 1541-1563.

Jones, A.G., Ledo, J., Ferguson, I.J., 2005a. Electromagnetic images of the Trans-Hudson orogen: The North American Central Plains anomaly revealed. Canadian Journal of Earth Sciences 42 (4), 457-478.

Jones, A.G. Ledo, J., Ferguson, I.J., Farquharson, C., Garcia, X., Grant, N., McNeice, G.W., Roberts, B., Spratt, J., Wennberg, G., Wolynec, L., Wu, X., 2005b. The electrical resistivity structure of Archean to Tertiary lithosphere along 3,200 km of SNORCLE profiles, northwestern Canada. Canadian Journal of Earth Sciences 42 (6), 1257-1275.

Jones, A.G. Lezaeta, P., Ferguson, I.J., Chave, A.D., Evans, R., Garcia, X., Spratt, J., 2003. The electrical structure of the Slave craton. Lithos 71 (2-4), 505-527.

Karato, S., 1990. The role of hydrogen in the electrical conductivity of the upper mantle. Nature 347 (6290), 272-273.

Karato, S., 2006. Remote sensing of hydrogen in Earth's mantle, Water in Nominally Anhydrous Minerals. Reviews in Mineralogy & Geochemistry. Mineralogical Society of America, Chantilly, 343-375.

Krajick, K., 2001. Barren Lands: An Epic Search for Diamonds in the North American Arctic. W. H. Freeman Company, 464 pp.

Ledo, J., Jones, A.G., 2005. Upper mantle temperature determined from combining mineral composition, electrical conductivity laboratory studies and magnetotelluric field observations: Application to the Intermontane belt, Northern Canadian Cordillera. Earth and Planetary Science Letters 236 (1-2), 258-268.

Li, A.B., Burke, K., 2006. Upper mantle structure of southern Africa from Rayleigh wave tomography. Journal of Geophysical Research-Solid Earth 111, 16, doi: 10.1029/2006JB004321.

McNeice, G.W., Jones, A.G., 2001. Multisite, multifrequency tensor decomposition of magnetotelluric data. Geophysics 66 (1), 158-173.

Muller, M.R., Jones, A.G., Evans, R.L., Grütter, H.S., Hatton, C., Garcia, X., Hamilton, M.P., Miensopust, M.P., Cole, P., Ngwisanyi, T., Hutchins, D., Fourie, C.J., Jelsma, H., Aravanis, T., Pettit, W., Webb, S.J., Wasborg, J., SAMTEX Team, 2009. Lithospheric structure, evolution and diamond prospectivity of the Rehoboth Terrane and western Kaapvaal Craton, southern Africa: constraints from broadband magnetotellurics. Lithos this volume.

Nguuri, T. K., Gore, J., James, D.E., Webb, S.J., Wright, C., Zengeni, T.G., Gwavava, O., Snoke, J.A., Kaapvaal Seismic Group, 2001. Crustal structure beneath southern Africa and its implications for the formation and evolution of the Kaapvaal and Zimbabwe cratons, Geophysical Research Letters 28 (13), 2501-2504.

Niblett, E.R., Sayn Wittgenstein, C., 1960. Variation of the electrical conductivity with depth by the magnetotelluric method. Geophysics 25 (5), 998-1008.

Park, S.K., Ducea, M.N., 2003. Can in situ measurements of mantle electrical conductivity be used to infer properties of partial melts? Journal of Geophysical Research-Solid Earth 108, doi: 10.1029/2002JB001899, 12 pp.

Simpson, F., Bahr, K., 2005. Practical magnetotellurics. Cambridge University Press, ISBN 0521817277, 9780521817271, 254 pp.

Vozoff, K. (Editor), 1986. Magnetotelluric Methods. Geophysics Reprint Series, 5. Society of Exploration Geophysicists, Tulsa, OK, U.S.A.

Webb, S., 2009. Southern African tectonics from potential field interpretation. Ph.D. thesis, University of the Witwatersrand, Johannesburg.

Wessel, P., Smith, W.H.F., 1991. Free software help map and display data. EOS Transactions AGU 72, 441.

Wessel, P., Smith, W.H.F., 1998. New, improved version of the Generic Mapping Tools released. EOS Transactions AGU 79, 579.

York, D., 1966. Least-squares fitting of a straight line. Canadian Journal of Physics 44 (5), 1079-1086.

York, D., 1969. Least squares fitting of a straight line with correlated errors. Earth and Planetary Science Letters 5 (5), 320-324.

Figure Captions

Figure 1: SAMTEX magnetotelluric station location map. The coloured circles show the locations of the stations in each of the four phases, plus data donated to SAMTEX by De Beers. The black circles are the station locations of the Kaapvaal Seismic Experiment. The tectonic subdivision is from Nguuri et al. (2001) and Webb (2009), and is based on known geology in South Africa and Zimbabwe, and primarily on interpretation of potential field data in Namibia and Botswana where thick Kalahari sands cover basement. Country boundaries are shown in dashed lines.

Figure 2: An image of the resistivity at 100 km depth based on an approximate transformation of the MT responses from period to depth and taking the maximum resistivity found (see text for details). The colours are $log_{10}(resistivity)$, and the black dots show stations at which data were used. At the P-T conditions for the Kaapvaal Craton mantle rocks comprising olivine, pyroxenes and garnet are expected to have a resistivity in excess of 30,000 Ω.m, i.e., blue.

Figure 3: An image of the resistivity at 200 km constructed in the same manner as Fig. 2. Also shown on the figure are kimberlite locations; red means known to be diamondiferous, green means known to be non-diamondiferous, and white means not defined or unknown.

Figure 4: An image of the magnitude of electrical anisotropy at 100 km depth, given by $log_{10}(\rho_{max}/\rho_{min})$. Regions that exhibit low orders of electrical anisotropy (less than a decade in orthogonal directions) are blue, and regions that exhibit high orders of anisotropy are light brown to white. Stations that contribute data to this image are shown as black dots.

Figure 5: An image of the magnitude of electrical anisotropy at 200 km depth, constructed in the same manner as Fig. 4. Kimberlite locations plotted with the same colour coding as Fig. 3.

Figure 6: The total integrated electrical conductivity, or conductance (S), from 40 km to 200 km. This depth range is approximately the mantle lithosphere from the average base of the crust to the average base of the lithosphere. The colours represent $log_{10}(S)$. For olivine-pyroxenes-garnet mineralogy at cratonic conditions the mantle lithospheric conductance should be of the order of 10 Siemens (purple). Also plotted are the kimberlite localities colour coded as in Fig. 3.

Figure 7: Shear wave seismic velocity at a depth of 100 km from a model constructed through inversion of fundamental mode Rayleigh wave arrivals (Li and Burke, 2006). Kimberlite locations plotted with the same colour coding as Fig. 3.

Figure 8: Comparison of the resistivity image at 200 km with the anomalous compressional velocities from models constructed through inversion of body wave arrivals (Fouch et al., 2004; James et al., 2001). The resistivities are plotted in *log10(resistivity)*, and the velocity perturbations are in terms of percentage difference from the average at that depth, with values between -0.25% and +0.25% set to transparent. Kimberlite locations plotted with the same colour coding as Fig. 3.

Figure 9: Comparison of the resistivity image at 200 km with the anomalous shear wave velocities from models constructed through inversion of body wave arrivals (Fouch et al., 2004; James et al., 2001). The resistivities are plotted in *log10(resistivity)*, and the velocity perturbations are in terms of percentage difference from the average at that depth, with values between -0.25% and +0.25% set to transparent. Kimberlite locations plotted with the same colour coding as Fig. 3.

Figures

Figure 1

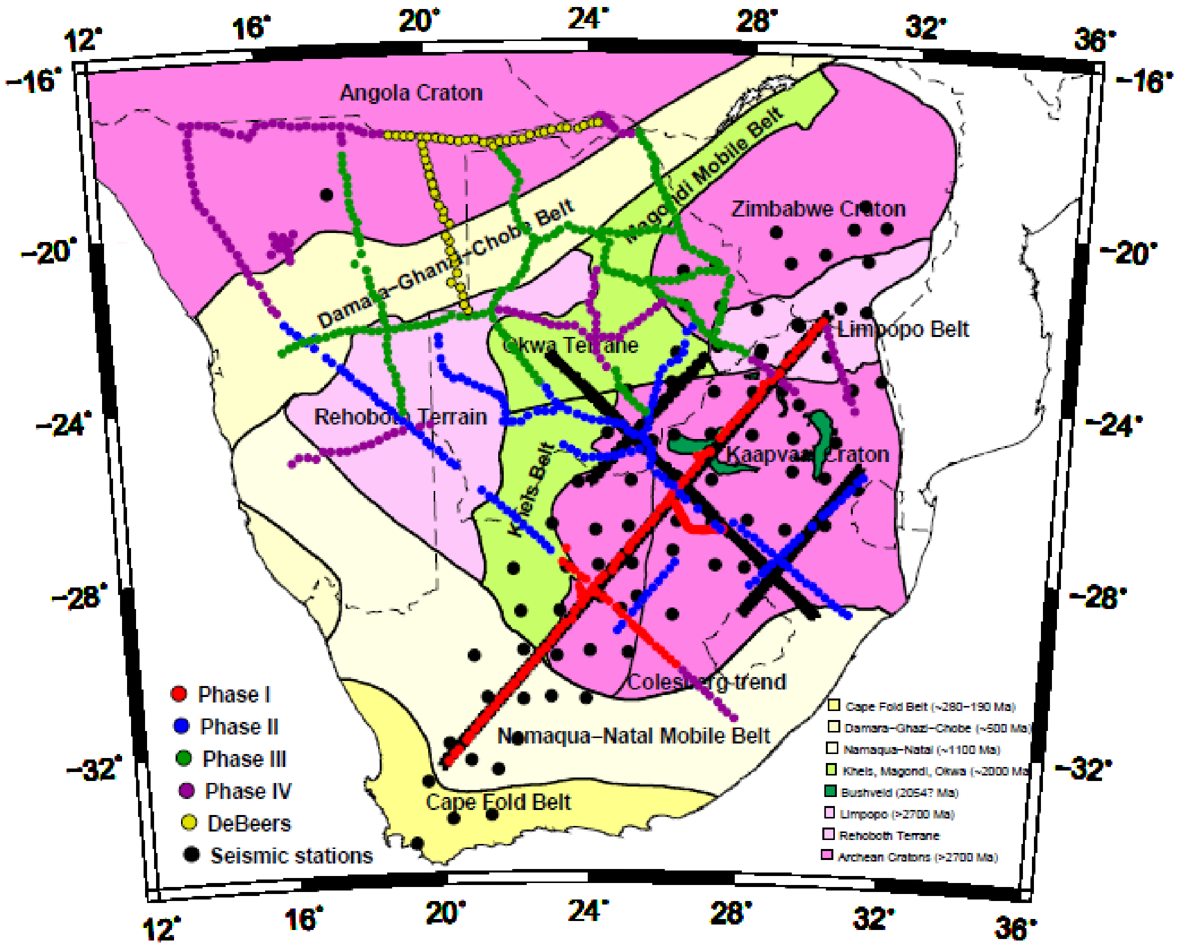

Figure 2 RhoMAX100km

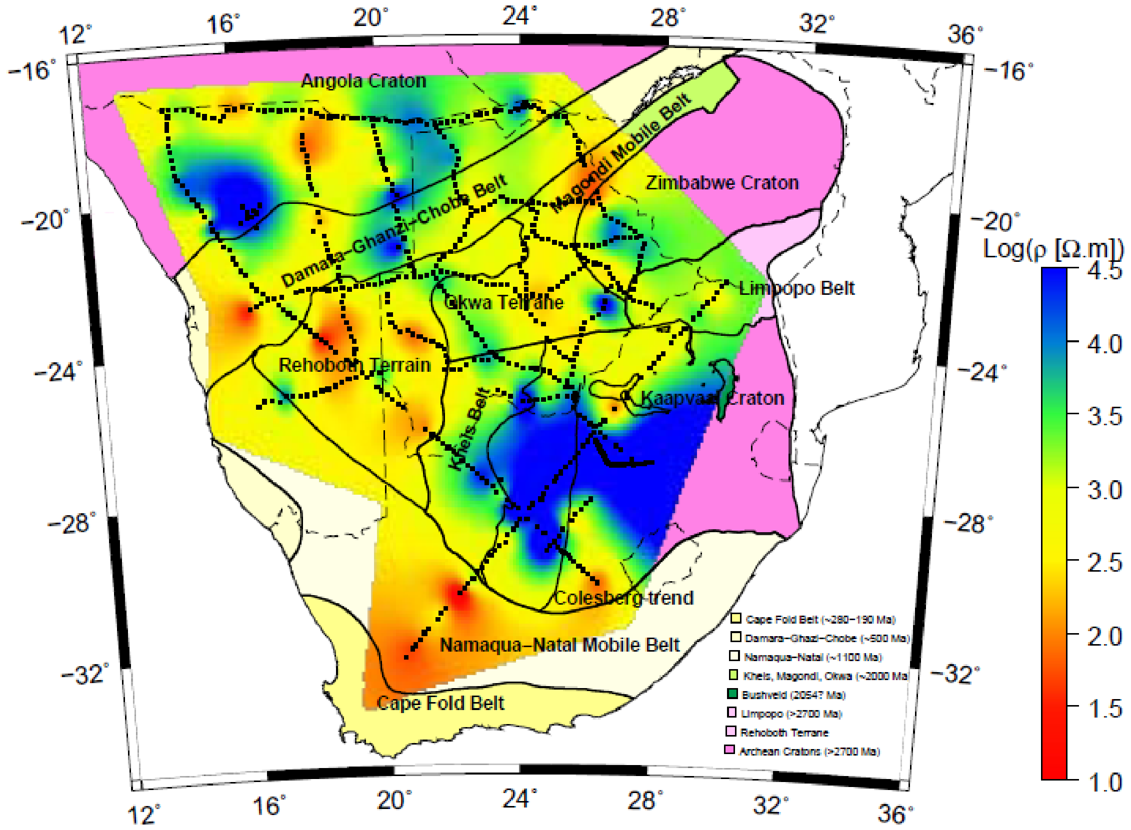

Figure 3: RhoMAX200km

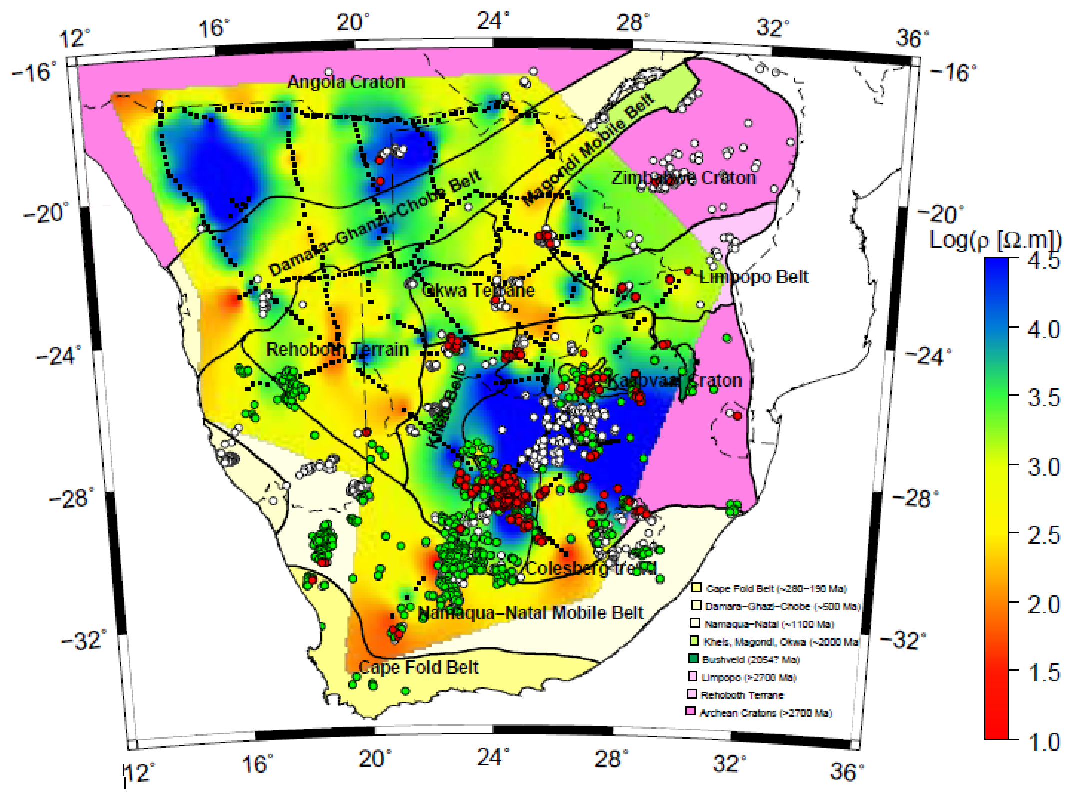

Figure 4: RhoANIS100km

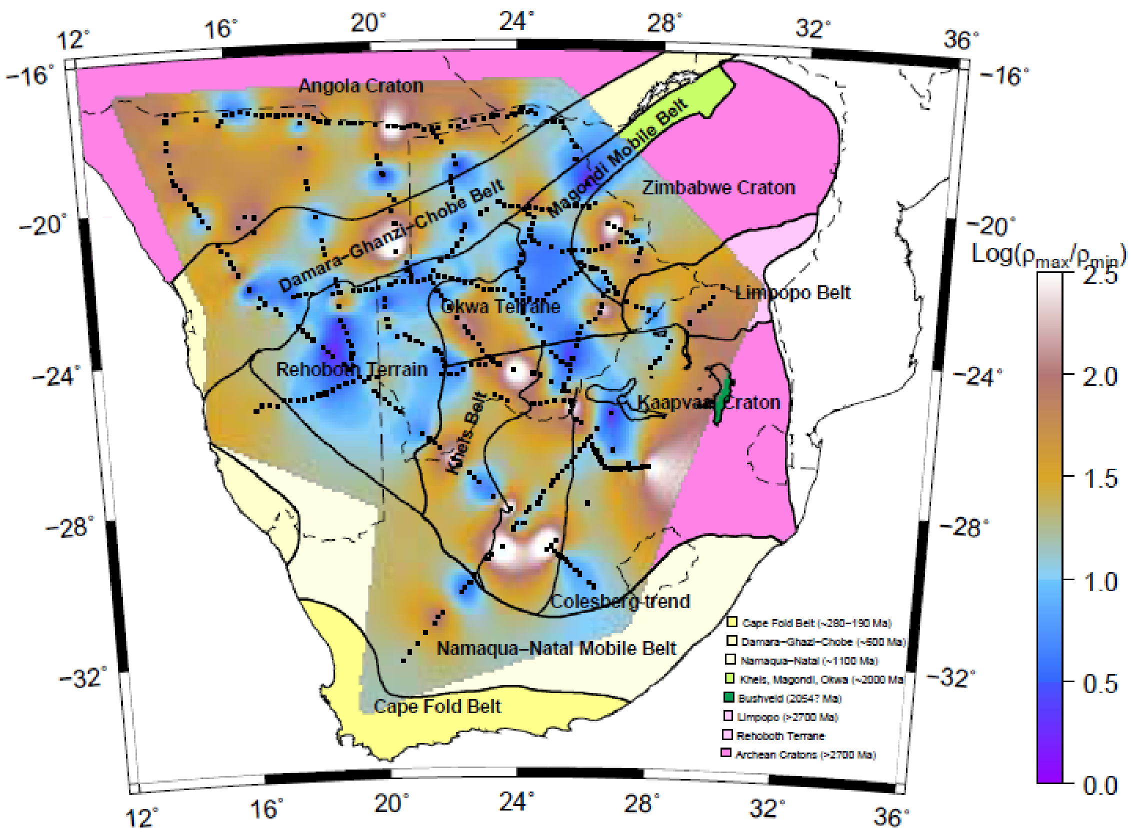

Figure 5: RhoANIS200km

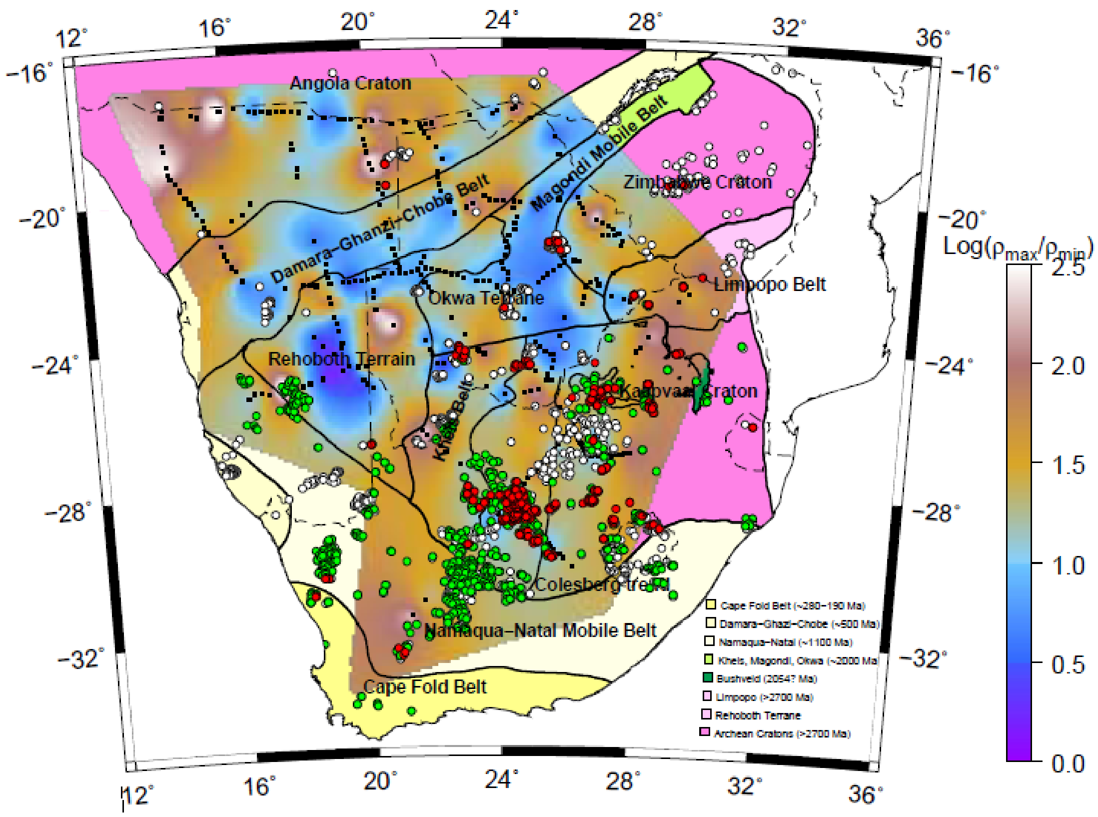

Figure 6: CondAV40-200km

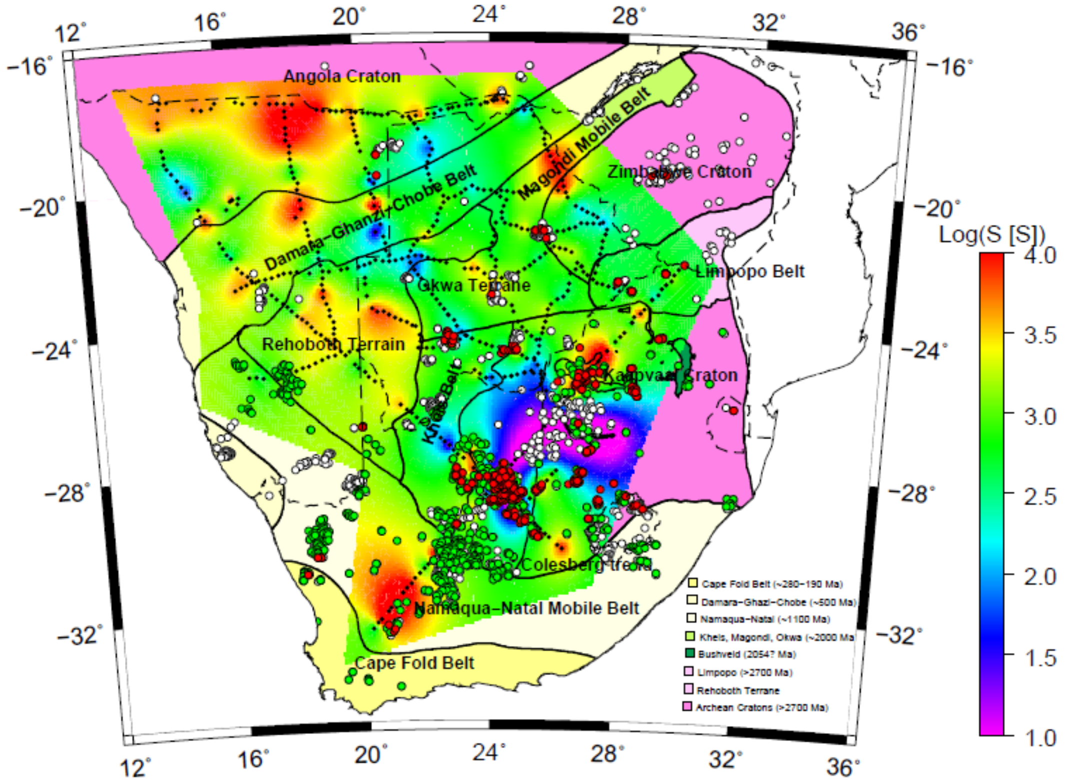

Figure 7: LiBurke80-100km

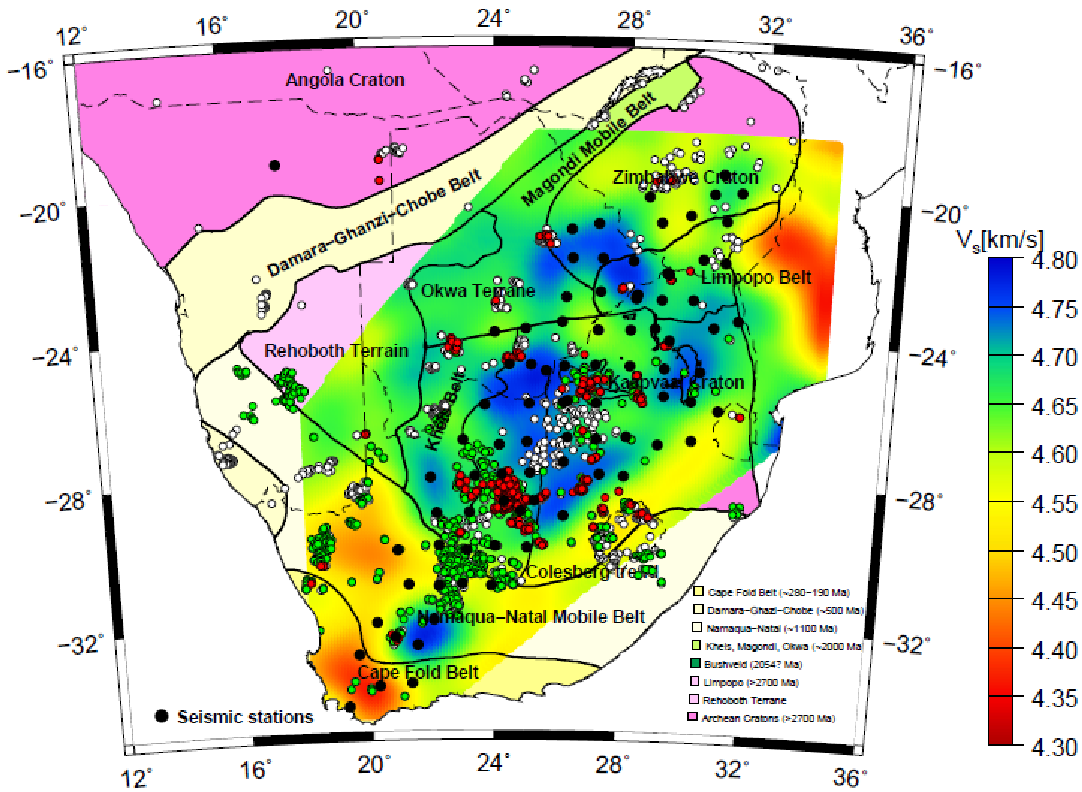

Figure 8: RhoFOuchP200km

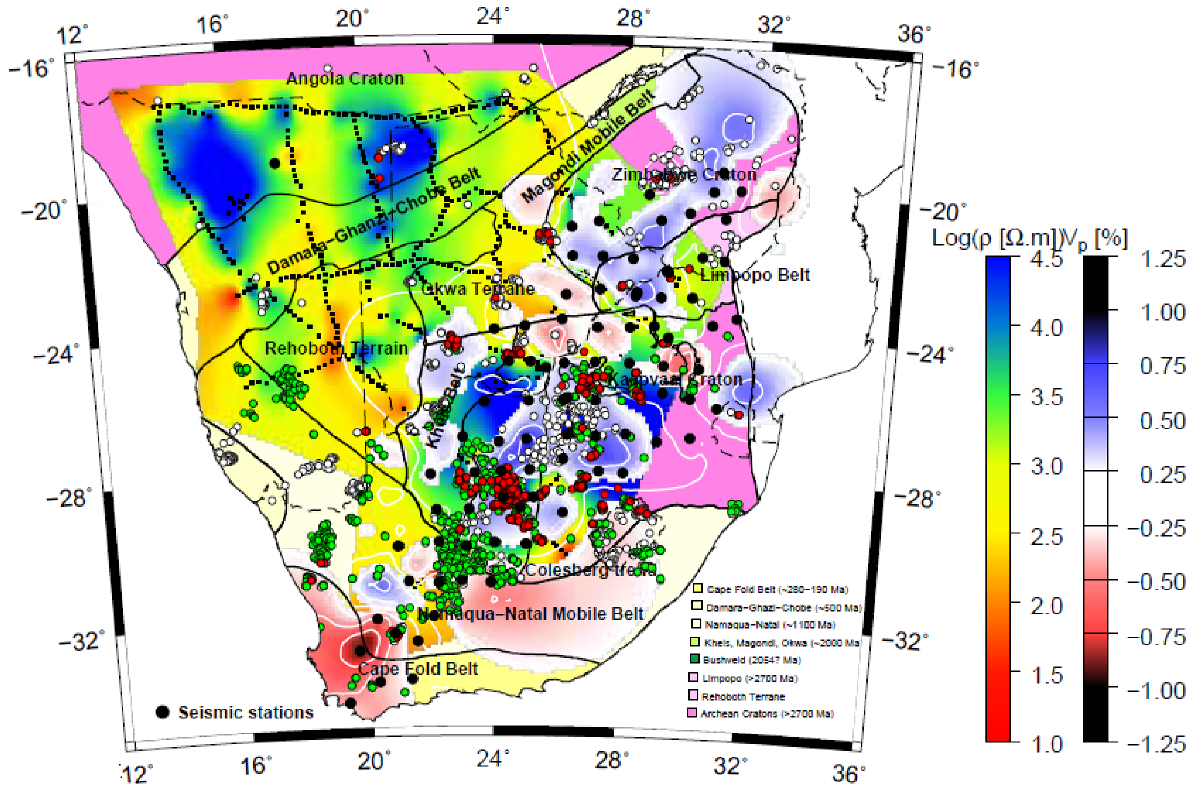

Figure9: RhoFouchS200km